

Construct, Merge, Solve & Adapt with Reinforcement Learning for the min–max Multiple Traveling Salesman Problem

Guillem Rodríguez-Corominas ^{1,2}, Maria J. Blesa ², and Christian
Blum ¹

¹Artificial Intelligence Research Institute (IIIA-CSIC), Bellaterra,
Catalunya, Spain, grodriguez@iiaa.csic.es,
christian.blum@iiaa.csic.es

²Universitat Politècnica de Catalunya (UPC), Barcelona, Catalunya,
Spain, maria.j.blesa@upc.edu

Abstract

The Multiple Traveling Salesman Problem (mTSP) extends the Traveling Salesman Problem to m tours that start and end at a common depot and jointly visit all customers exactly once. In the min–max variant, the objective is to minimize the longest tour, reflecting workload balance. We propose a hybrid approach, *Construct, Merge, Solve & Adapt* with Reinforcement Learning (RL-CMSA), for the symmetric single-depot min–max mTSP. The method iteratively constructs diverse solutions using probabilistic clustering guided by learned pairwise q -values, merges routes into a compact pool, solves a restricted set-covering MILP, and refines solutions via inter-route remove, shift, and swap moves. The q -values are updated by reinforcing city-pair co-occurrences in high-quality solutions, while the pool is adapted through ageing and pruning. This combination of exact optimization and reinforcement-guided construction balances exploration and exploitation. Computational results on random and TSPLIB instances show that RL-CMSA consistently finds (near-)best solutions and outperforms a state-of-the-art hybrid genetic algorithm under comparable time limits, especially as instance size and the number of salesmen increase.

Keywords: Multiple Traveling Salesman Problem, Construct, Merge, Solve & Adapt, Reinforcement Learning

1 Introduction

The Multiple Traveling Salesman Problem (mTSP) generalizes the TSP to m tours that start and end at a common depot and collectively visit each customer exactly once. It can be viewed as a simplified vehicle routing problem (VRP) without vehicle capacities or time windows [11, 7]. Two objectives are usually considered: (i) minimizing total traversal cost (the *min-sum mTSP*) and (ii) minimizing the length of the longest tour among the m tours (the *min-max mTSP*). The min-max criterion is particularly relevant when balancing workload or service time is important, as in last-mile delivery with identical vehicles, coordinated multi-robot patrolling, UAV sortie planning, or technician routing, where fairness and service-level constraints are crucial [14]. This paper focuses on the single-depot min-max mTSP on symmetric graphs, a setting that captures many practical applications while remaining computationally challenging.

Formally, let $G = (V, E)$ be a complete undirected graph with $V = \{0, 1, \dots, n\}$, where 0 denotes the depot and D_{ij} is the metric cost of edge (i, j) . The task is to construct m closed routes $\{\mathcal{R}_1, \dots, \mathcal{R}_m\}$ that (i) are node-disjoint except for the depot, (ii) cover $\{1, \dots, n\}$ exactly once, and (iii) minimize $\max_{k=1, \dots, m} \text{len}(\mathcal{R}_k)$, where $\text{len}(\cdot)$ is the tour cost. The problem is NP-hard even for metric instances by reduction from the TSP and balanced partitioning arguments. Consequently, exact algorithms scale only to modest sizes, while heuristics and metaheuristics dominate large-instance practice.

In recent years, hybrid metaheuristics that combine heuristic search with exact optimization components have shown strong potential for tackling difficult combinatorial problems. Along these lines, we build on the *Construct, Merge, Solve & Adapt* (CMSA) framework, which is itself a hybrid metaheuristic integrating constructive solution generation with an exact solving phase. In particular, we consider its Reinforcement Learning extension, RL-CMSA [8], which augments standard CMSA with a Q-learning mechanism to guide and adapt key decisions during the search. We argue that this additional learning-driven adaptation can be especially beneficial for the problem studied in this paper.

2 Related Work

Methodologically, mTSP algorithms largely follow the standard routing taxonomy: *exact* approaches (e.g., branch-and-cut on arc/flow models with

subtour elimination, or set-partitioning with branch-and-price) and *heuristics/metaheuristics* that trade optimality guarantees for scalability [10, 13]. Within the latter, two recurring design patterns are *cluster-first route-second* (assign customers to m salesmen via balanced partitioning methods and then solve m TSPs) and *route-first cluster-second* (build a giant tour and optimally *split* it into m routes via shortest-path or dynamic-programming procedures) [5]. Modern hybrids strengthen these templates with powerful local search (e.g., 2-opt/Or-opt/ k -exchange), tailored recombination, and diversity control, often yielding state-of-the-art performance in both min-sum and min-max settings.

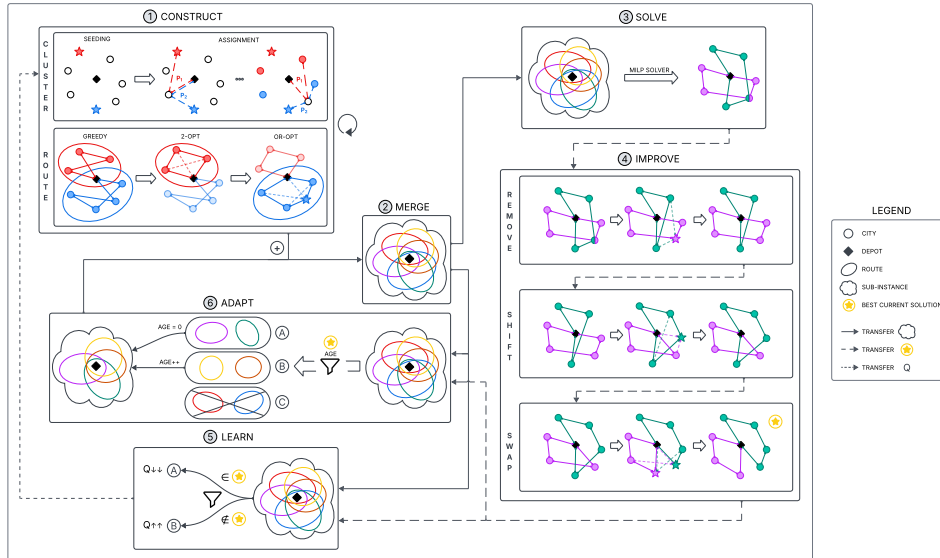


Figure 1: RL-CMSA: Schematic Algorithm Overview

Genetic Algorithms are particularly prominent in the mTSP literature, evolving either explicit multi-route representations or TSP-like permutations with route delimiters, combined with selection and diversity mechanisms and typically hybridized with local improvement [4]. For the min-max mTSP, a strong representative is the Hybrid Genetic Algorithm (HGA) of [5], which encodes solutions as TSP sequences, evaluates individuals through a DP-based *Split* tailored to the min-max objective, and combines a similarity-aware crossover with both inter- and intra-route local search (e.g., 1-shift/1-swap/Or-opt/2-opt), plus intersection handling. When tested on four standard benchmark suites—including, for example, TSPLIB instances and ran-

dom instances—the HGA achieves state-of-the-art average performance under comparable cutoffs and improves best-known results on a substantial subset of instances, making it a leading baseline for our setting. Therefore, in this paper, we study the min–max mTSP under the same modeling assumptions and use the HGA as a strong baseline for comparison.

Beyond GAs, mTSP variants have been tackled by Ant Colony Optimization [15], Artificial Bee Colony [12], Invasive Weed Optimization [13], General Variable Neighborhood Search [10], and Memetic Algorithms [14, 2], to name a few. For the min–max variant, competitive examples include the Hybrid Search with Neighborhood Reduction (HSNR) [1], which alternates tabu-based inter-tour moves with EAX-based intra-tour improvement; and the Iterated Two-Stage Heuristic (ITSHA) [16], combining randomized or clustering-based initialization with variable neighborhood improvement (2-opt/insert/swap).

Finally, Reinforcement Learning (LR) and GNN-based methods have emerged as promising alternatives. Notable examples include multi-agent RL frameworks (e.g., ScheduleNet) [6] and Neuro–Cross Exchange (NCE), which learns to activate a cross-exchange neighborhood [3]. These methods can produce competitive solutions quickly, though classical/hybrid metaheuristics still dominate many standard benchmarks under typical time budgets.

3 The Proposed Algorithm

A schematic overview of our RL-CMSA algorithm is given in Figure 1. The algorithm iterates through six phases—*Construct*, *Merge*, *Solve*, *Improve*, *Learn*, and *Adapt*—until the stopping criterion is met (here, a time limit). In the following sections, all algorithm components are explained in detail.

3.1 Construct

In the first phase of the algorithm, we generate $n_{\text{solutions}}$ candidate solutions through a probabilistic construction process. Each construction is divided into two stages: CLUSTER and ROUTE.

CLUSTER stage: The goal of this stage is to partition the set of cities V (excluding the depot) into m clusters, one for each vehicle. The intuition is that cities that are likely to belong to the same route should be grouped together. Algorithm 1 provides pseudocode for this procedure.

The clustering process begins by selecting m *centers*, which serve as the initial representatives for each cluster (see **Seeding**). These centers are chosen using a k -means++ style seeding procedure, biased by the q -values of city pairs (see lines 1-12 of Algorithm 1):

1. The first center is sampled from the non-depot cities with probability proportional to the squared distance from the depot.
2. Each subsequent center is chosen using a roulette-wheel selection, where the probability of selecting a city i depends on its squared distance to the nearest already-chosen center, adjusted by the corresponding q -value.

This ensures that centers are both well separated and more likely to belong to different optimal routes. Figure 1 illustrates this process, where the chosen centers are marked with a star.

After the centers are chosen, the remaining cities are assigned to clusters (**Assignment**). The so far unassigned cities from U are then assigned one by one to the clusters using a weighted assignment mechanism (see lines 13-32 of Algorithm 1). Cities with smaller angular distance (with respect to the depot) to a center ($\text{angdist}(\theta_u, \theta_{c_j})$) are more likely to be processed earlier. For each candidate city u , we compute the approximate assignment cost into each cluster C_j , defined as the distance to its two closest points in that cluster, including the depot when applicable (function `TWOCLOSESTPOINTS()`). When scoring the assignment of a city u into a cluster C_j (see line 26), we scale the cost by two additional factors: (i) the *mean Q -compatibility* between u and all current members of C_j , excluding the depot (see line 24), and (ii) a *running estimate* $r_{u,j}$ of how the max length would increase if the city is added to this cluster (see line 25).¹ Note that a small $\varepsilon > 0$ is added for numerical stability.

Once the costs are computed, with probability $d_{\text{rate}}^{\text{construct}}$, the city is assigned to the cluster with the lowest score. Ties are broken uniformly at random using reservoir sampling. Otherwise, the cluster is chosen with probabilities $p_j \propto \frac{1}{s_j}$. The factor L_j^{approx} is updated incrementally after each insertion using the corresponding two-anchor insertion cost, which implicitly encourages *load balancing* by penalizing already long provisional routes.

This procedure is repeated until all cities have been assigned to clusters.

¹Note that $d_{u,j}$ and L_j^{approx} are proxies computed from anchor distances and are used only to guide clustering. Actual tours are constructed in the subsequent ROUTE stage.

Algorithm 1: Clustering algorithm biased by q -values

Input: D : pairwise distances; Q : q -values; m : # routes

Output: $\mathcal{R} = \{C_1, \dots, C_m\}$: m clusters

```
1 Phase 1: Seeding
2 Initialize  $U \leftarrow V \setminus \{0\}$ ; // Non-depot cities
3 Initialize  $w_i \leftarrow D_{0,i}^2$  for all  $i \in U$ ;
4 for  $j = 1$  to  $m$  do
5   | Sample center  $c_j \in U$  with probability  $\propto w_i$ ;
6   |  $U \leftarrow U \setminus \{c_j\}$ ;
7   | Initialize cluster  $C_j \leftarrow \{0, c_j\}$ ;
8   | Initialize  $L_j^{\text{approx}} \leftarrow 2 \cdot D_{0,c_j}$ ;
9   | foreach  $i \in U$  do
10  | |  $w_i \leftarrow \min\{w_i, D_{i,c_j}^2 \cdot Q_{i,c_j}^2\}$ ;
11  | end
12 end

13 Phase 2: Assignment
14 foreach  $u \in U$  do
15  |  $\delta_u \leftarrow \min_{j=1, \dots, m} \text{angdist}(\theta_u, \theta_{c_j})$ ;
16 end
17 while  $U \neq \emptyset$  do
18  | Sample city  $u \in U$  with probability  $\propto 1/\delta_u$ ;
19  |  $U \leftarrow U \setminus \{u\}$ ;
20  |  $L_{\max}^{\text{approx}} \leftarrow \max_{j=1, \dots, m} L_j^{\text{approx}}$ ;
21  | foreach  $j = 1, \dots, m$  do
22  | |  $\{a, b\} \leftarrow \text{TWOCLOSESTPOINTS}(u, C_j, D)$ ;
23  | |  $d_{u,j} \leftarrow D_{u,a} + D_{u,b} - D_{a,b}$ ;
24  | |  $q_{u,j}^{\text{mean}} \leftarrow \frac{1}{|C_j \setminus \{0\}|} \sum_{v \in C_j, v \neq 0} Q_{u,v}$ ;
25  | |  $r_{u,j} \leftarrow \max(L_{\max}^{\text{approx}}, L_j^{\text{approx}} + d_{u,j}) / L_{\max}^{\text{approx}}$ ;
26  | |  $s_j \leftarrow (d_{u,j} + \varepsilon) \cdot r_{u,j} \cdot q_{u,j}^{\text{mean}}$ ;
27  | end
28  | With probability  $d_{\text{rate}}^{\text{construct}}$ : choose  $j^* \in \arg \min_j s_j$ ;
29  | Otherwise: sample  $j^*$  with probability  $p_j \propto 1/s_j$ ;
30  |  $C_{j^*} \leftarrow C_{j^*} \cup \{u\}$ ;
31  |  $L_{j^*}^{\text{approx}} \leftarrow L_{j^*}^{\text{approx}} + d_{u,j^*}$ ;
32 end
33 return  $\mathcal{R} = \{C_1, \dots, C_m\}$ ;
```

ROUTE stage: Once the clustering is complete, we build one route per cluster using a fast greedy insertion heuristic. Starting from the depot, we construct a tour for each cluster using best-insertion into the partial route. The resulting tour is then improved by applying intra-route local search: first a 2-opt procedure and then an Or-opt procedure restricted to relocating sequences of length 1 and 2. Both local searches scan candidate moves in random order and apply first improvement, to avoid systematic bias. This produces high-quality cluster tours at low computational cost.

After all routes of a solution have been constructed, we apply the inter-route improvement operators described in Section 3.4. To reduce computational cost, we restrict the neighborhood to moves involving the longest route only, rather than considering all route pairs.

By repeating the above procedure $n_{\text{solutions}}$ times, RL-CMSA generates a set of $n_{\text{solutions}}$ solutions to the problem.

3.2 Merge

Next, in the *Merge* step of RL-CMSA (see the center of Figure 1), the $n_{\text{solutions}} \times m$ routes generated in the *Construct* step are added to the pool $\mathcal{R}_{\text{cand}}$ of candidate routes. Each route stored in $\mathcal{R}_{\text{cand}}$ is assigned an *age* value, which is initialized to 0 upon insertion.²

Since the construction process may generate multiple routes visiting the same set of non-depot cities, we keep only one representative per visited-city set, namely the shortest one. To do so, we compute a canonical signature for each route by sorting its non-depot cities. This signature is then used for hashing and equality checks when inserting into $\mathcal{R}_{\text{cand}}$.

Finally, we prune $\mathcal{R}_{\text{cand}}$ by discarding any route whose length exceeds the current incumbent max-route length. Such routes will never be selected by the solver (as explained in the following section), and keeping them would only bias the subsequent learning step.

3.3 Solve

After the *Merge* step, RL-CMSA conducts the *Solve* step (top right of Figure 1) to determine the best solution that can be assembled from the candidate pool $\mathcal{R}_{\text{cand}}$. We formulate a *set-covering* MILP that selects exactly m routes while ensuring that every non-depot city is covered at least

²This will be important for the *Adapt* step explained in Section 3.6.

once, and minimizes the length of the longest selected route. The resulting subproblem is solved with **CPLEX**, a state-of-the-art MILP solver.

More formally, let $x_r \in \{0, 1\}$ be a binary variable indicating whether route $r \in \mathcal{R}_{\text{cand}}$ is selected, and let z be an upper bound on the maximum length among selected routes. The model is:

$$\begin{aligned}
\min \quad & z \\
\text{s.t.} \quad & z \geq \ell_r - M(1 - x_r) && \forall r \in \mathcal{R}_{\text{cand}} \\
& \sum_{r \in \mathcal{R}_{\text{cand}}} x_r = m \\
& \sum_{r \ni i} x_r \geq 1 && \forall i \in V \setminus \{0\}
\end{aligned}$$

where ℓ_r denotes the length of route r and M is a sufficiently large constant. Note that not forcing each city to be covered by only one route allows for greater flexibility. However, as the selected routes may overlap, the output $\mathcal{R}_{\text{best}}$ is not necessarily a valid mTSP solution yet, and duplicates are resolved in the subsequent *Improve* step. Note that we can impose z to be bounded by the current incumbent best solution, which justifies pruning such routes from $\mathcal{R}_{\text{cand}}$ in the previous step.

3.4 Improve

In the *Improve* step of RL-CMSA (see bottom right in Figure 1), $\mathcal{R}_{\text{best}}$ is refined by applying a series of local improvement operations to its routes. The primary objective is to minimize the length of the longest route in $\mathcal{R}_{\text{best}}$, henceforth denoted by z .

3.4.1 Remove

This step turns $\mathcal{R}_{\text{best}}$ into a feasible solution (if necessary) by removing non-depot cities occurring in more than one route in the following way.

For each duplicated city, we evaluate the potential decrease in route length that would result from removing the city from a given route by directly connecting its predecessor and successor. Let u denote the city to be removed, and let a and b be its predecessor and successor in the route, respectively. The *removal improvement* Δ_{remove} is defined as

$$\Delta_{\text{remove}}(u) = D_{au} + D_{ub} - D_{ab} \quad .$$

Once these improvement values have been computed for all duplicated cities across all routes, we proceed as follows: with probability $d_{\text{rate}}^{\text{improve}}$, we remove

the city yielding the highest removal improvement; otherwise, we select a city to remove using a roulette-wheel mechanism, with probabilities proportional to their respective Δ_{remove} values. These values are scaled by the respective current route length to prioritize deletions from longer routes. This process is repeated iteratively until every non-depot city appears in exactly one route.

3.4.2 Shift: cross-route relocation (1-move)

Aiming for further improvement, we attempt to *shift* a single city u across routes, that is, to relocate it from its current source route into some position within a different target route of $\mathcal{R}_{\text{best}}$. The goal of this operation is to reduce the total route length by moving cities that are poorly placed, i.e., far from their neighboring cities, into routes that are closer. For all eligible cities and insertion positions, the following values are computed:

$$\Delta_{\text{src}}^-(u) = D_{au} + D_{ub} - D_{ab} \quad (\text{removal gain}),$$

$$\Delta_{\text{tgt}}^+(p, u) = D_{cu} + D_{ud} - D_{cd} \quad (\text{insertion cost}),$$

where a and b are the predecessor and successor of u in its source route, and (c, d) denotes the edge at the target insertion position p . Therefore, a relocation move has a net value given by:

$$\Delta_{\text{shift}} = \Delta_{\text{src}}^-(u) - \Delta_{\text{tgt}}^+(p, u) \quad ,$$

and is considered *admissible* only if the maximum route length after applying the move does not exceed z . Note that, with $\Delta_{\text{shift}} > 0$, the move strictly improves the secondary objective (total length), so it is unambiguously beneficial.

Since the primary objective is to minimize the length of the longest route in $\mathcal{R}_{\text{best}}$, we also allow admissible moves with $\Delta_{\text{shift}} < 0$: these may slightly increase the total length but still improve the main objective. To balance exploitation and exploration, we select among admissible moves as follows: with probability $d_{\text{rate}}^{\text{improve}}$ we select the best move; otherwise we sample a move via roulette-wheel with probabilities proportional to $\exp(\frac{\Delta_{\text{shift}}}{z})$. This weighting favors moves that reduce both z and the total length ($\Delta_{\text{shift}} > 0$), while still giving a small but nonzero chance to moves with $\Delta_{\text{shift}} < 0$ when they reduce z , our primary objective. After applying the chosen move, only the affected Δ values around the modified positions are incrementally updated. This repeats iteratively until no admissible relocation remains.

3.4.3 Swap: cross-route exchange (1–1 swap)

In this phase, we attempt to *swap* two cities u and v belonging to different routes from $\mathcal{R}_{\text{best}}$, r_{src} and r_{tgt} ($\text{src} \neq \text{tgt}$), respectively. The objective is to further reduce route lengths by exchanging cities that may be better suited to each other’s routes. The incremental cost of such a swap is evaluated locally around the affected positions in each route. Let a and b denote the predecessor and successor of u in r_{src} , and c and d those of v in r_{tgt} . The respective local cost variations are computed as:

$$\Delta_{\text{src}}(u \leftrightarrow v) = (D_{au} + D_{ub}) - (D_{av} + D_{vb}),$$

$$\Delta_{\text{tgt}}(u \leftrightarrow v) = (D_{cv} + D_{vd}) - (D_{cu} + D_{ud}).$$

The total gain from performing the swap is then given by:

$$\Delta_{\text{swap}} = \Delta_{\text{src}}(u \leftrightarrow v) + \Delta_{\text{tgt}}(u \leftrightarrow v).$$

Similarly to the shift move, a swap is considered *admissible* only if the maximum route length after applying the swap does not exceed z . Furthermore, we also allow moves with $\Delta_{\text{swap}} \leq 0$ if they improve the maximum route length z . Again, we select the swap with the maximum Δ_{swap} with probability $d_{\text{rate}}^{\text{improve}}$. Otherwise, we sample a move using a roulette wheel with probabilities proportional to $\exp(\frac{\Delta_{\text{swap}}}{z})$. After applying the swap, only the cost entries in the neighborhoods of the modified positions are incrementally updated. The process repeats iteratively until no admissible improving swap moves remain.

The final solution $\mathcal{R}_{\text{best}}$ is the current best solution of RL-CMSA. This solution is marked in Figure 1 with a golden, encircled, asterisk. It serves as input to the *Learn* and *Adapt* steps, as explained below.

3.5 Learn

We estimate two symmetric co-occurrence counts over unordered pairs $\{i, j\}$ of non-depot cities:

$$S_{\text{cand}}(i, j) = \#\{\text{routes in } \mathcal{R}_{\text{cand}} \text{ containing both } i, j\}$$

$$S_{\text{best}}(i, j) = \#\{\text{routes in } \mathcal{R}_{\text{best}} \text{ containing both } i, j\}$$

In other words, $S_{\text{best}}(i, j)$ evaluates to either zero or one. For pairs that appear in the candidate pool ($S_{\text{cand}}(i, j) > 0$), the following update of the

corresponding q -values is conducted:

$$Q_{ij} \leftarrow \begin{cases} Q_{ij} - l_{\text{rate}} \cdot Q_{ij}, & \text{if } S_{\text{best}}(i, j) > 0 \quad (\text{reinforce}) \\ Q_{ij} + l_{\text{rate}} \cdot (1 - Q_{ij}), & \text{if } S_{\text{best}}(i, j) = 0 \quad (\text{discourage}). \end{cases}$$

Thus, beneficial pairs drift toward 0 (more likely to end up in the same cluster in the *Construct* step), while unhelpful pairs drift toward 1. Moreover, a convergence proxy $\frac{2}{(n-1)(n-2)} \sum_{i < j} |\frac{1}{2} - Q_{ij}|$ is monitored over a short time window. If it stagnates, we reset all q -values to 0.5 and clear the sub-instance.

3.6 Adapt

In the *Adapt* step of RL-CMSA (see center left of Figure 1), the sub-instance $\mathcal{R}_{\text{cand}}$ is updated using an age-based policy. Routes in $\mathcal{R}_{\text{best}}$ that are not yet in $\mathcal{R}_{\text{cand}}$ are inserted with age 0. Conversely, the age of each route in $\mathcal{R}_{\text{cand}}$ that is not part of $\mathcal{R}_{\text{best}}$ is increased by one. Finally, any route whose age reaches the threshold age_{max} is removed. This policy bounds the size of $\mathcal{R}_{\text{cand}}$, promotes turnover, and keeps the pool compact and up-to-date with the evolving reinforcement signal.

4 Experimental Evaluation

The RL-CMSA algorithm described in the previous section stops at a user-defined computation time limit. It returns the best solution found. To assess the behaviour and applicability of our approach, we compare it with the state-of-the-art HGA algorithm from [5]. All experiments were performed on the ARS MAGNA computing cluster at IIIA-CSIC (Intel Xeon 2.2 GHz, 10 cores, 92 GB RAM). For each instance, both algorithms were executed with a time limit of n seconds (the number of cities).

4.1 Benchmark Instances

We considered two types of benchmark instances. First, and most importantly, we used randomly generated instances. Random instances are the most-used ones in the mTSP literature; however, for the min-max mTSP, they may become unintentionally easy when one or a few cities lie far from the depot. In such cases—especially as the number of vehicles increases—the optimal solution often consists of a few-city route to visit the distant

city (or cities), while the remaining routes cover only nearby cities. To mitigate this effect and obtain more challenging instances, we generated random instances as follows: city locations are sampled uniformly at random inside a circle of radius 1, placing the depot at the centre. This construction increases the likelihood that several cities lie near the boundary and thus at comparable distances from the depot. We generated 20 random instances for each $n \in \{50, 100, 200\}$. All these instances will be solved for $m \in \{\frac{1}{100}n, \frac{5}{100}n, \frac{10}{100}n, \frac{15}{100}n\}$. In other words, the number of salesmen considered (m) depends on the number of cities (n) and is calculated as 1%, 5%, 10% or 15% of the number of cities (rounded).

Second, we also considered instances from TSPLIB, which are commonly used in related work. In particular, we used `eil51`, `berlin52`, `eil76`, and `rat99`. These instances allow us to evaluate our approach on structured, well-known benchmarks and to test its behaviour across different problem characteristics.

4.2 Algorithm Tuning

To ensure good performance of our algorithm, a scientific parameter tuning was performed using I-RACE, an automatic algorithm configuration tool. In particular, parameter tuning was performed independently for each considered value of m (see above). For each m , a training set of five additional random instances with 200 nodes (the largest size considered) was generated.

Table 1: Summary of the parameters of RL-CMSA with their respective domain and the tuning results.

Parameters	Considered Domain	Tuning results			
		$m = 1\%$	$m = 5\%$	$m = 10\%$	$m = 15\%$
$n_{\text{solutions}}$	$\{2, 3, \dots, 19, 20\}$	19	17	13	17
$d_{\text{rate}}^{\text{construct}}$	$\{0.00, 0.01, \dots, 0.89, 0.90\}$	0.87	0.83	0.66	0.86
$d_{\text{rate}}^{\text{improve}}$	$\{0.00, 0.01, \dots, 0.99, 1.00\}$	0.96	0.97	0.98	0.93
l_{rate}	$\{0.10, 0.11, \dots, 0.49, 0.50\}$	0.31	0.26	0.45	0.20
age_{max}	$\{2, 3, \dots, 19, 20\}$	12	13	2	15

Table 1 reports the parameter domains explored by I-RACE and the best configurations obtained. Overall, a clear pattern emerges for $m \in \{1\%, 5\%, 15\%\}$: both $n_{\text{solutions}}$ and age_{max} take relatively large values, suggesting that maintaining a larger sub-instance is beneficial. In addition, l_{rate} is set to a medium value, indicating that the algorithm tends to learn more slowly. Concerning the determinism rates, $d_{\text{rate}}^{\text{construct}}$ and $d_{\text{rate}}^{\text{improve}}$ are high (the latter is close to 1), which implies that newly constructed solutions are

kept close to the current best solution. This behaviour is consistent with an intensification strategy: the algorithm focuses the search in the neighbourhood of the best-so-far solution, and retaining a large sub-instance helps include routes similar to the incumbent, enabling a more thorough local exploration.

In contrast, the configuration found for $m = 10$ differs substantially. Here, $n_{\text{solutions}}$ takes a more moderate value and age_{max} is very small, which leads to smaller sub-instances and a shorter retention of seemingly bad routes. Combined with a lower value of $d_{\text{rate}}^{\text{construct}}$, this indicates a stronger emphasis on diversification: the algorithm generates more diverse candidates and keeps only the highest-quality ones. Moreover, the relatively high l_{rate} suggests faster convergence.

For the HGA algorithm, we used the parameter values reported by the authors in [5]. These values were tuned on a diverse set of instances, including random instances and the TSPLIB instances considered in this study.

4.3 Results

Tables 2(a)-(d) summarize the comparative results of RL-CMSA and HGA for each value of m on the random instances. Each row corresponds to one instance (identified by `id`). For each problem size $n \in \{50, 100, 200\}$, the tables report, separately for RL-CMSA and HGA, the average objective value over 40 independent runs (`mean`), the number of runs in which the method achieved the best value among the two compared algorithms (`#b`), and the average time in seconds for finding the best solution of a run (`time`). In addition, the last column of each table block (regarding n and m) reports the best objective value obtained on that instance across all runs and both algorithms (`best`). Boldface highlights the best `mean` value between the two algorithms for the corresponding instance and size, while the shaded cells provide a visual cue of which method performs better (blue for RL-CMSA, red for HGA, and grey for ties). The arrow and bolt symbols indicate, respectively, which algorithm attains a higher best-runs count and which one is faster for the corresponding instance, following the same color pattern.

Table 2: Summary of the obtained results on random instances.

id	50												100												200											
	HGA			RL-CMSA			HGA			RL-CMSA			HGA			RL-CMSA			HGA			RL-CMSA														
	mean	#b	time	mean	#b	time	best	mean	#b	time	best	mean	#b	time	best	mean	#b	time	best	mean	#b	time	best													
0	5.075160	40	0.87	5.075160	40	0.04	5.075160	7.015623	39	5.60	7.015623	40	1.41	7.015623	9.070852	2	92.60	9.690439	0	87.50	9.632396															
1	5.370131	40	1.52	5.370131	40	0.09	5.370131	6.843089	40	6.88	6.843089	40	0.34	6.843089	9.391857	11	96.76	9.318625	1	77.57	9.316580															
2	5.331649	40	1.38	5.331649	40	0.04	5.331649	7.029934	40	12.08	7.029934	40	2.25	7.029934	9.424885	2	61.20	9.420873	4	86.93	9.400750															
3	5.286716	40	1.27	5.286716	40	0.04	5.286716	6.974608	27	26.94	6.982347	40	1.91	6.982347	9.460975	1	84.20	9.481597	0	86.02	9.481420															
4	5.281849	40	1.39	5.281849	40	0.31	5.281849	6.534432	40	2.57	6.534432	40	0.51	6.534432	9.3270634	30	61.71	9.350576	2	96.43	9.308409															
5	5.577140	40	13.71	5.577140	40	0.17	5.577140	7.652171	38	17.69	7.6921997	40	0.50	7.6921997	9.5010956	21	3.44	9.576244	0	100.38	9.504786															
6	5.436203	40	1.77	5.436203	40	0.21	5.436203	6.774343	37	20.44	6.774343	40	0.25	6.774343	9.417832	5	98.84	9.4047427	0	107.28	9.380471															
7	5.186137	39	1.51	5.186137	40	0.05	5.186137	7.174352	2	17.13	7.146589	40	3.27	7.146589	9.841626	1	78.96	9.8202728	0	109.07	9.791297															
8	5.2554913	40	1.70	5.2554913	40	0.17	5.2554913	7.1174241	40	23.65	7.1174241	40	1.87	7.1174241	9.0895254	25	72.83	9.514759	0	88.74	9.682829															
9	5.0439071	40	1.89	5.0439071	40	0.18	5.0439071	6.850206	38	3.39	6.8501996	40	0.19	6.8501996	9.9153469	1	47.17	9.9314959	1	102.36	9.920767															
10	5.458819	40	2.25	5.458819	40	0.11	5.458819	6.985233	33	41.22	6.9754031	40	0.11	6.9754031	9.426128	0	92.06	9.40005	9	90.95	9.387241															
11	5.1127317	40	2.85	5.1127317	40	0.32	5.1127317	7.308773	3	16.61	7.2842068	40	0.93	7.2842068	9.456790	0	53.46	9.4410405	8	92.25	9.389246															
12	5.1685487	40	1.56	5.1685487	40	0.07	5.1685487	7.175547	35	21.11	7.1736817	40	0.25	7.1736817	9.4298983	0	80.09	9.449652	1	103.29	9.402946															
13	5.441950	40	1.34	5.441950	40	0.08	5.441950	7.103581	37	19.57	7.1009282	40	0.39	7.1009282	9.661714	2	106.89	9.5883556	0	96.15	9.551736															
14	5.4295509	40	1.35	5.4295509	40	0.41	5.4295509	7.527059	9	19.66	7.5128586	40	15.50	7.5128586	9.7290299	19	74.67	9.794566	0	99.37	9.734294															
15	5.2143740	40	1.28	5.2143740	40	0.07	5.2143740	7.0079489	40	6.27	7.0079489	40	0.63	7.0079489	9.670111	25	54.16	9.6640371	29	97.16	9.659729															
16	4.926863	40	1.37	4.926863	40	0.04	4.926863	6.624747	23	20.07	6.6541699	40	8.98	6.6541699	9.6199999	19	52.40	9.670741	0	113.18	9.590847															
17	5.5142674	40	1.53	5.5142674	40	0.08	5.5142674	7.312478	16	33.06	7.3033378	40	11.32	7.3033378	9.7192209	4	81.64	9.727120	0	95.28	9.697934															
18	5.5010121	40	1.91	5.5010121	40	0.03	5.5010121	7.037797	38	5.22	7.0377289	40	1.40	7.0377289	9.511951	0	49.63	9.5168366	7	98.41	9.511777															
19	5.3125777	40	1.25	5.3125777	40	0.07	5.3125777	7.158301	12	25.53	7.1452419	40	8.18	7.1452419	10.0551592	9	101.97	10.1035920	0	96.50	10.039911															

(a) Results for $m = 1%$

id	50												100												200											
	HGA			RL-CMSA			HGA			RL-CMSA			HGA			RL-CMSA			HGA			RL-CMSA														
	mean	#b	time	mean	#b	time	best	mean	#b	time	best	mean	#b	time	best	mean	#b	time	best	mean	#b	time	best													
0	3.860317	40	1.31	3.860317	40	0.05	3.860317	3.922935	31	14.73	3.930727	40	12.85	3.930727	2.727857	0	68.43	2.7174812	1	79.86	2.714117															
1	3.889238	40	2.39	3.889238	40	1.86	3.889238	3.850106	5	40.50	3.858642	36	29.56	3.858642	2.632363	0	81.83	2.637016	1	79.28	2.633184															
2	3.9158255	40	1.27	3.9158255	40	0.04	3.9158255	3.2843014	40	9.64	3.2843014	40	1.23	3.2843014	2.6194326	0	95.05	2.5987804	1	59.89	2.597280															
3	3.7164153	40	1.29	3.7164153	40	0.08	3.7164153	3.288724	36	7.54	3.2875303	40	0.60	3.2875303	2.6720860	0	83.89	2.632805	4	96.35	2.655052															
4	3.771724	40	1.40	3.771724	40	0.07	3.771724	3.1388556	15	11.44	3.1265507	40	6.11	3.1265507	2.6468459	0	79.90	2.6385345	2	85.81	2.632597															
5	3.8417454	40	1.48	3.8417454	40	0.05	3.8417454	3.417398	22	26.93	3.4120586	40	6.11	3.4120586	2.6646631	8	50.16	2.6547707	34	72.79	2.654120															
6	3.8581195	40	1.76	3.8581195	40	0.16	3.8581195	3.270115	39	14.86	3.2681905	40	2.13	3.2681905	2.6411771	20	56.21	2.6326352	32	77.57	2.632692															
7	3.8385517	40	1.56	3.8385517	40	0.08	3.8385517	3.344050	30	18.01	3.3407747	40	2.13	3.3407747	2.734475	20	85.32	2.7178544	34	79.15	2.716874															
8	3.819252	40	1.49	3.819252	40	0.15	3.819252	3.371203	27	6.85	3.370511	40	2.59	3.370511	2.705522	0	52.76	2.6929041	8	100.25	2.685182															
9	3.7176965	40	5.11	3.7176965	40	0.10	3.7176965	3.329353	8	8.73	3.2973346	40	3.75	3.2973346	2.6987361	1	67.23	2.6881647	1	92.08	2.687179															
10	3.877639	37	1.25	3.877639	40	0.04	3.877639	3.3301308	13	2.44	3.3269885	40	1.02	3.3269885	2.6646970	0	96.51	2.657440	1	113.00	2.645914															
11	3.7106351	40	2.83	3.7106351	40	0.26	3.7106351	3.441860	29	6.61	3.4334664	40	1.40	3.4334664	2.6117045	30	70.40	2.6114520	40	15.54	2.6114520															
12	3.8366626	40	1.38	3.8366626	40	0.05	3.8366626	3.320073	9	1.96	3.3818698	40	0.42	3.3818698	2.6651408	6	83.31	2.6504960	33	77.98	2.6509865															
13	3.9645314	40	1.38	3.9645314	40	0.05	3.9645314	3.417927	26	35.69	3.4151308	40	14.95	3.4151308	2.6479474	7	85.45	2.6443881	1	52.76	2.6333981															
14	3.9277470	40	1.38	3.9277470	40	0.09	3.9277470	3.4166408	33	10.49	3.4126897	40	3.21	3.4126897	2.7196794	0	88.24	2.6916992	2	65.02	2.6881828															
15	3.7609393	40	1.32	3.7609393	40	0.04	3.7609393	3.414278	7	30.22	3.4062272	40	6.59	3.4062272	2.7188663	6	74.90	2.7143756	4	68.39	2.708578															
16	3.6615327	40	3.06	3.6615327	40	0.30	3.6615327	3.3211292	3	9.83	3.3172333	23	33.57	3.3171375	2.674608	3	83.87	2.6620640	40	59.85	2.662940															
17	3.8902231	40	1.26	3.8902231	40	0.04	3.8902231	3.456541	0	7.81	3.4337737	10	16.01	3.4337963	2.6989833	16	62.60	2.6882923	12	75.08	2.680392															
18	4.002660	37	9.65	4.002660	40	0.98	4.002660	3.321423	35	36.26	3.3217752	40	1.69	3.3217752	2.6586214	11	87.76	2.6368782	34	75.10	2.6369368															
19	3.8903967	40	3.21	3.8903967	40	0.47	3.8903967	3.374201	21	31.61	3.3513830	40	5.83	3.3513830	2.7352698	1	70.14	2.7275546	0	69.25	2.718531															

(b) Results for $m = 3%$

id	50												100												200											
	HGA			RL-CMSA			HGA			RL-CMSA			HGA			RL-CMSA			HGA			RL-CMSA														
	mean	#b	time	mean	#b	time	best	mean	#b	time	best	mean	#b	time	best	mean	#b	time	best	mean	#b	time	best													
0	2.757461	40	2.74	2.757461	40	0.08	2.757461	2.368136	4	4.39	2.3619281	10	41.93	2.3573197	2.1192907	0	35.27	2.1188193	40	63.00	2.1188193															
1	2.7528314	40	1.27	2.7528314	40	0.06	2.7528314	2.5719676	25	30.78	2.5610634	40	3.80	2.5610634	2.1137251	0	84.29	2.1071810	2	69.32	2.104938															
2	2.792029	11	9.57	2.792066	40	1.47	2.792066	2.292916	32																											

while HGA no longer attains a best-found solution consistently across runs, RL-CMSA still does, yielding better average objective values. For larger instances ($n = 100$ and $n = 200$), RL-CMSA more regularly achieves better average objective values than HGA; the main exception occurs for $m = 1\%$ (see Table 2(a)), where HGA seems to outperform RL-CMSA on the largest instances ($n = 200$). Note that the number of runs producing a best-found solution (**#b**) is an indication of algorithm robustness. For $n = 50$ and $n = 100$, RL-CMSA reaches a best-found solution for almost all instances and in nearly all of the 40 executions, indicating very stable performance. For $n = 200$, RL-CMSA initially struggles to match the best solution frequently (particularly for small m), but this behaviour greatly improves as m increases: the **#b** counts grow with m , and for $m = 15\%$ RL-CMSA again reaches the best solution in almost all runs for most instances.

Finally, regarding running times, RL-CMSA is consistently faster for $n = 50$ and $n = 100$, reaching its best obtained solutions within noticeably lower CPU times than HGA. For $n = 200$, the comparison depends on m : for $m = 1\%$ HGA is generally faster, for $m \in \{5\%, 10\%\}$ both methods exhibit similar running times (with instance-dependent differences), and for $m = 15\%$ RL-CMSA becomes faster in most instances. Overall, these results show that RL-CMSA dominates in average objective value and best-run frequency for almost all settings, with the main drawback appearing for the largest instances when m is small. With increasing m , RL-CMSA improves both robustness and runtime on large instances and becomes the preferred option.

The weaker performance of RL-CMSA for small values of m can be explained by the intrinsic mechanics of the method. As m increases, tours become shorter, which makes the *Solve* step more effective: the sub-instance contains shorter route components that can be recombined in many feasible ways, increasing the number of promising route combinations and thus facilitating the construction of high-quality solutions. In other words, a given sub-instance offers greater combinatorial flexibility when routes are short. In contrast, when m is very small, routes are necessarily much longer and substantially harder to combine. Consequently, the *Solve* step provides less benefit. This also explains why the tuning process tends to favour larger sub-instances in this setting: retaining a bigger pool of routes increases the chance of including routes that can be combined into a competitive solution.

Table 3: Statistical tests comparing RL-CMSA vs HGA, paired by instance.

n	50		100		200	
	r_{rb}	p -value	r_{rb}	p -value	r_{rb}	p -value
1%	0.0000	1.000e+00	-1.0000	4.883e-04 ^{***}	0.3714	5.000e-01
5%	-1.0000	1.000e+00	-1.0000	4.196e-05 ^{***}	-1.0000	2.289e-05 ^{***}
10%	-1.0000	5.000e-01	-1.0000	2.747e-04 ^{***}	-0.8762	1.175e-03 ^{**}
15%	-1.0000	3.906e-02 [*]	-0.8242	3.662e-02 [*]	-1.0000	4.196e-05 ^{***}

Table 3 summarises the paired statistical comparison between RL-CMSA and HGA for each combination of $m \in \{1\%, 5\%, 10\%, 15\%\}$ and problem size $n \in \{50, 100, 200\}$. For each instance, we compute the mean objective value over the 40 independent runs of each algorithm and then apply a paired Wilcoxon signed-rank test across instances. The table reports the rank-biserial correlation r_{rb} as an effect-size measure and the corresponding Holm-corrected p -values. Negative values of r_{rb} indicate that RL-CMSA tends to obtain better performance than HGA, and viceversa.

These statistical results confirm that RL-CMSA is statistically superior in most settings. For $n = 100$, RL-CMSA significantly outperforms HGA for all considered values of m , with very large effect sizes ($r_{rb} = -1$) and corrected p -values below 0.05. For $n = 200$, the advantage is also significant for $m \in \{5\%, 10\%, 15\%\}$, again with large negative effect sizes, whereas for $m = 1\%$ the difference is not significant and the effect size favours HGA. For $n = 50$, a significant difference is only observed for $m = 15\%$, whereas for $m \in \{1\%, 5\%, 10\%\}$ the comparison is not significant after correction. This indicates that, on the smallest instances and for smaller values of m , HGA and RL-CMSA behave similarly.

To better understand why RL-CMSA tends to produce more consistent results than HGA, we analyze a Search Trajectory Network (STN) [9] built from all executions of both algorithms on instance id=17 with $n = 200$ and $m = 10\%$ (a large instance with a medium-high number of vehicles). Figure 2 depicts the trajectories followed by the two methods during the search. Each node corresponds to one or more solutions visited during an execution, and each directed edge indicates a transition to better solutions. Node colours follow the same scheme as in Table 2, while grey nodes represent solutions visited by both algorithms. Yellow squares indicate initial solutions, and black triangles represent the final solutions of each run. The best solutions found are highlighted with a red circle; note that, as in the mTSP, it is very common that multiple different solutions share the same best objective value. The vertical position of a node encodes solution quality

(fitness): higher nodes correspond to worse solutions, whereas lower nodes correspond to better ones. Since the STN is displayed with perspective, some black triangles may appear higher than the red-circled nodes depending on the viewpoint, although the red nodes correspond to the best solutions found. It can be observed that HGA typically starts from a narrow set of similar initial solutions and then disperses over a broader portion of the search space; several runs approach the region of high-quality solutions, but they rarely reach the best solutions. In contrast, RL-CMSA starts from more diverse initial solutions (often of better quality) and, in most runs, rapidly converges towards the same region where the best-found solutions are located. This behaviour suggests that RL-CMSA is more effective at guiding the search towards promising search space areas, which in turn explains its higher robustness across runs.

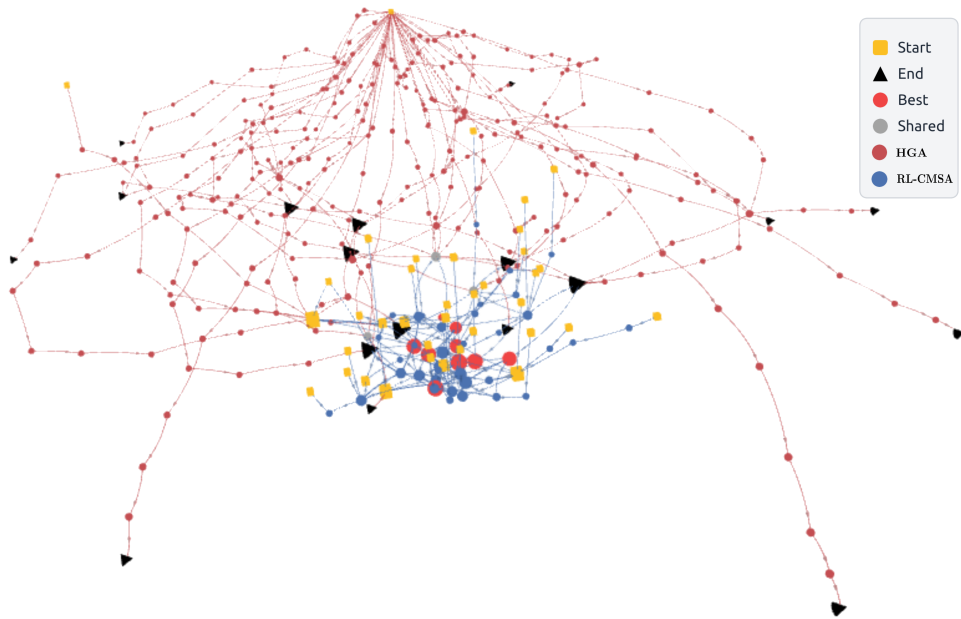


Figure 2: STN graphic regarding instance 17 with $n = 200$ and $m = 10\%$.

Figure 3 shows the distribution of the pairwise structural distances between the 40 solutions obtained by each algorithm on each of the 20 problem instances (with $n = 200$ and $m = 10\%$) using violinplots. Again, HGA is colored red, while RL-CMSA is colored blue. Wider regions of a violin indicate that many distances fall in that range, while the overlaid box/whiskers summarize the central tendency and spread (median and interquartile range),

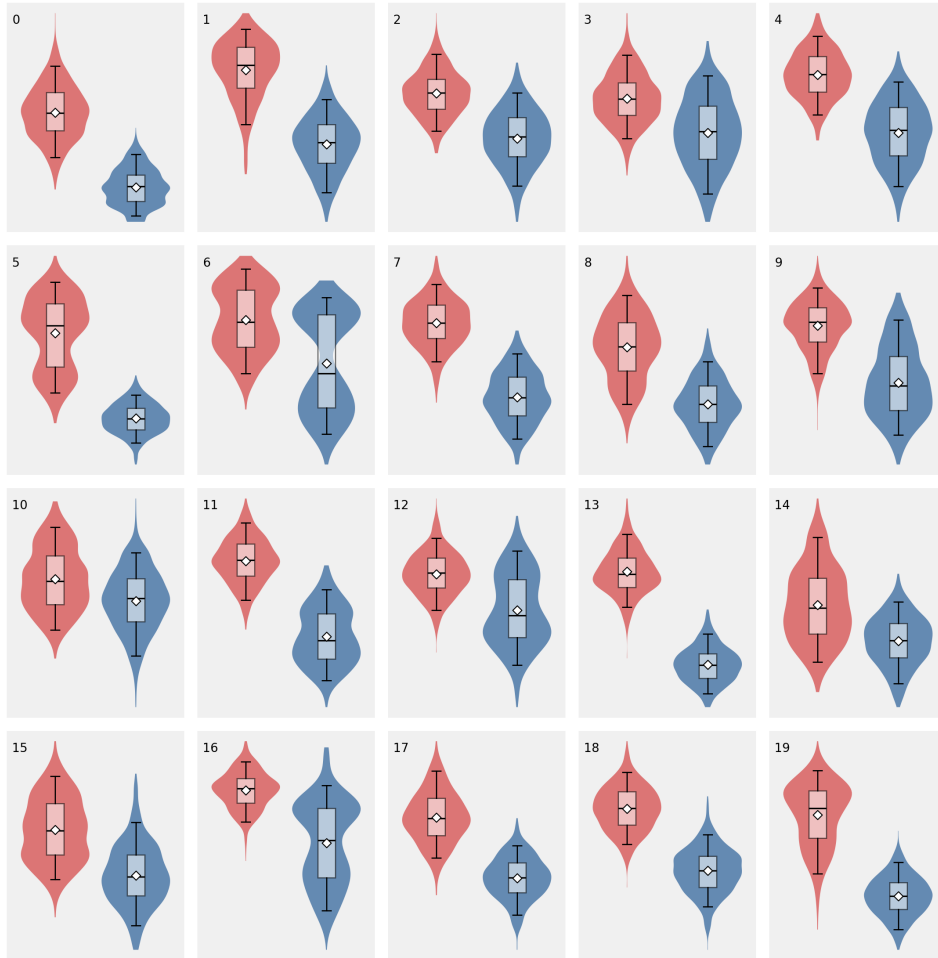


Figure 3: Structural distances between the 40 best-found solutions per run (and per algorithm) for the 20 problem instances with $n = 200$ and $m = 10\%$.

helping compare how dispersed the obtained solutions are for each method on each instance. Overall, a clear pattern emerges: HGA tends to produce solutions that are more different to each other (the red violins are usually shifted upward and often wider), which indicates higher diversity / more scattered search trajectories. In contrast, RL-CMSA typically produces solutions more similar among each other with tighter distributions (blue violins are generally lower and narrower). This is consistent with what was

observed in the context of the STN graphic of Figure 2.

Table 4: Summary of the obtained results for the TSPLIB instances.

n	e1251				ber11802				e1176				rat99							
	HGA		RL-CMSA		HGA		RL-CMSA		HGA		RL-CMSA		HGA		RL-CMSA					
	mean	#b	mean	#b	best	mean	#b	best	mean	#b	best	mean	#b	best	mean	#b	best			
1%	222.75794	37	222.73337	40个	222.73337	4110.21310	40个	4110.21310	40个	4110.21310	281.22379	25	280.85394	40个	280.85394	665.99090	40个	665.99090	40个	665.99090
5%	159.37151	40个	159.37151	40个	159.37151	3069.58569	40个	3069.58569	40个	3069.58569	159.50091	40个	159.50091	40个	159.50091	430.33361	0	430.29462	24个	430.27258
10%	118.13375	40个	118.13375	40个	118.13375	2440.92196	40个	2440.92196	40个	2440.92196	127.56175	39	127.56175	40个	127.56175	436.44014	40个	436.44014	40个	436.44014
15%	112.07141	40个	112.07141	40个	112.07141	2440.92196	40个	2440.92196	40个	2440.92196	127.56175	40个	127.56175	40个	127.56175	436.44014	40个	436.44014	40个	436.44014

Finally, Table 4 reports results on the TSPLIB instances using the same summary format as before. Here, the four horizontal blocks correspond to the tested instances (ordered by increasing size), and rows to the different m values. Overall, RL-CMSA matches HGA’s mean objective in most settings and improves it in five of them. It achieves the best-known solution in all executions except for one case (rat99 with $m = 5\%$), where it still reaches the best in more than half of the runs. The table omits the time to reach the best-found solutions due to space limitations. Nonetheless, RL-CMSA is generally faster than HGA. The few exceptions coincide with settings where RL-CMSA is also stronger in solution quality, suggesting that additional search time can help it escape local optima and converge to better solutions.

5 Conclusions and Future Work

In this paper, we introduced RL-CMSA, a hybrid *Construct–Merge–Solve–Adapt* framework with reinforcement-guided clustering for the min–max mTSP. The method generates diverse candidate solutions, maintains a compact pool of high-quality routes, and repeatedly solves a restricted set-covering MILP to recombine them, while updating pairwise q -values to bias future constructions. On randomly generated instances, RL-CMSA is robust and generally improves both the mean objective value and the frequency of best runs compared to the state-of-the-art HGA. These gains are statistically significant in most settings, and become more pronounced as the number of cities and vehicles increases. The main exception occurs on the largest instances when the number of routes is very small. Moreover, on the considered TSPLIB instances, RL-CMSA outperforms HGA in five settings. In the remaining cases, the two methods achieve comparable results, although RL-CMSA is generally faster. An analysis of the search dynamics further indicates that RL-CMSA tends to drive runs toward a single high-quality region, yielding more consistent outcomes, whereas HGA explores more broadly and exhibits greater run-to-run variability.

As future work, we will strengthen RL-CMSA by enriching the route pool, e.g., by integrating additional large-scale neighborhoods, and by extending the reinforcement scheme to learn higher-order route features beyond pairwise co-occurrences. We also plan to evaluate the approach on broader and larger benchmark families and to extend it to more general routing settings with additional constraints.

Acknowledgements

This work was supported in part by the Department of Research and Universities of the Government of Catalonia by means of an European Social Fund (ESF)-Founded Pre-Doctoral Grant of the Catalan Agency for Management of University and Research Grants (AGAUR) under Grant 2022 FI_B 00903, in part by the Agencia Estatal de Investigación (AEI) under grants PID-2020-112581GB-C21 (MOTION) and PID2022-136787NB-I00 (ACISUD), and in part by the European Commission–NextGenerationEU, through Momentum CSIC Programme: Develop Your Digital Talent, under Project MMT24-IIIA-02.

References

- [1] Pengfei He and Jin-Kao Hao. Hybrid search with neighborhood reduction for the multiple traveling salesman problem. *Computers & Operations Research*, 142:105726, June 2022.
- [2] Pengfei He and Jin-Kao Hao. Memetic search for the minmax multiple traveling salesman problem with single and multiple depots. *European Journal of Operational Research*, 307(3):1055–1070, June 2023.
- [3] Minjun Kim, Junyoung Park, and Jinkyoo Park. Neuro cross exchange: Learning to cross exchange to solve realistic vehicle routing problems, 2022.
- [4] Jun Li, Qirui Sun, MengChu Zhou, and Xianzhong Dai. A new multiple traveling salesman problem and its genetic algorithm-based solution. In *2013 IEEE International Conference on Systems, Man, and Cybernetics*, page 627–632. IEEE, October 2013.
- [5] Sasan Mahmoudinazlou and Changhyun Kwon. A hybrid genetic algorithm for the min–max multiple traveling salesman problem. *Computers & Operations Research*, 162:106455, February 2024.

- [6] Junyoung Park, Sanjar Bakhtiyar, and Jinkyoo Park. Schedulenet: Learn to solve multi-agent scheduling problems with reinforcement learning, 2021.
- [7] Yang-Byung Park. A hybrid genetic algorithm for the vehicle scheduling problem with due times and time deadlines. *International Journal of Production Economics*, 73(2):175–188, September 2001.
- [8] Jaume Reixach and Christian Blum. How to improve “construct, merge, solve and adapt”? use reinforcement learning! *Annals of Operations Research*, September 2024.
- [9] Camilo Chacón Sartori, Christian Blum, and Gabriela Ochoa. Stnweb: A new visualization tool for analyzing optimization algorithms. *Software Impacts*, 17:100558, 2023.
- [10] Banu Soylu. A general variable neighborhood search heuristic for multiple traveling salesmen problem. *Computers & Industrial Engineering*, 90:390–401, December 2015.
- [11] Lixin Tang, Jiying Liu, Aiying Rong, and Zihou Yang. A multiple traveling salesman problem model for hot rolling scheduling in shanghai baoshan iron & steel complex. *European Journal of Operational Research*, 124(2):267–282, July 2000.
- [12] Minghao Tong, Zhenhua Peng, and Qin Wang. A hybrid artificial bee colony algorithm with high robustness for the multiple traveling salesman problem with multiple depots. *Expert Systems with Applications*, 260:125446, January 2025.
- [13] Pandiri Venkatesh and Alok Singh. Two metaheuristic approaches for the multiple traveling salesperson problem. *Applied Soft Computing*, 26:74–89, January 2015.
- [14] Yongzhen Wang, Yan Chen, and Yan Lin. Memetic algorithm based on sequential variable neighborhood descent for the minmax multiple traveling salesman problem. *Computers & Industrial Engineering*, 106:105–122, April 2017.
- [15] Majid Yousefikhoshbakh and Mohammad Sedighpour. A combination of sweep algorithm and elite ant colony optimization for solving the multiple traveling salesman problem. *Proceedings of the Romanian Academy, Series A*, 13(4):295–301, 2012.

- [16] Jiongzhi Zheng, Yawei Hong, Wenchang Xu, Wentao Li, and Yongfu Chen. An effective iterated two-stage heuristic algorithm for the multiple traveling salesmen problem. *Computers & Operations Research*, 143:105772, July 2022.